

## TECHNOLOGICAL IMPROVEMENTS IN THE DARHT II ACCELERATOR CELLS \*

Ben A. Prichard, Jr.<sup>‡</sup>, J. Barraza<sup>†</sup>, M. Kang<sup>†</sup>, K. Nielsen<sup>†</sup>, F. Bieniosek<sup>#</sup>, K. Chow<sup>#</sup>, W. Fawley<sup>#</sup>,  
E. Henestroza<sup>#</sup>, L. Reginato<sup>#</sup>, W. Waldron<sup>#</sup>, R. Briggs<sup>♦</sup>, T. Hughes<sup>■</sup>, T. Genoni<sup>■</sup>

### Abstract

The DARHT facility will employ two perpendicular electron Linear Induction Accelerators to produce intense, bremsstrahlung x-ray pulses for flash radiography. The second axis, DARHT II [1], features an 18 MeV, 2-kA, 2-microsecond pulse accelerator. DARHT II accelerator cells have undergone a series of testing and modeling efforts to fully understand their unacceptable initial failure rate. These R&D efforts are part of the DARHT 2<sup>nd</sup> Axis Refurbishment and Commissioning project, and they have led to a better understanding of Linear Induction Accelerator technology and physics for the unique DARHT II design. Specific improvements have been identified and tested. Improvements in the cell oil region, the cell vacuum region, and the Pulse Forming Networks (PFNs) have been implemented in the prototype units that have doubled the cell's performance. The prototype acceptance tests have been completed, and the lifetime reliability requirements were exceeded. The shortcomings of the previous design are summarized. The improvements to the original design, their resultant improvement in performance, and various test results are included.

### INTRODUCTION

The DARHT II accelerator cells were originally outfitted with voltage monitors that were later found to be non-linear, resulting in the cells being tested at ~18% below the specified 193 kV. After monitors were replaced and voltage levels corrected, performance shortcomings were discovered in both the cell oil region and the cell vacuum region. Figure 1 shows a cross-section of the original cell design.

In the oil region, most high voltage breakdowns occurred on the outer edge of the Metglas [2] cores, in the upper quadrant of the cells. The majority of the damage was between core 4 and the high voltage plate, or between core 3 and core 4. Some standoffs or hockey pucks between the high voltage plate and end plate also suffered damage.

In the vacuum region, both insulator flashover and cathode to anode breakdown were observed. One instance of possible bulk insulator failure was observed. The insulator material, Mycalex [3], was chosen on the basis

of its electrical, vacuum, and mechanical properties. Vacuum breakdown included faults during the accelerating pulse and faults after the accelerating pulse during reversal.

The R&D effort to solve these problems was initially divided into oil region studies and vacuum region studies. After solutions were found, integrated studies were undertaken. The effort culminated in the prototype design acceptance testing where six modified cells underwent lifetime testing, demonstrating that the specified reliability of the refurbished cells was exceeded.

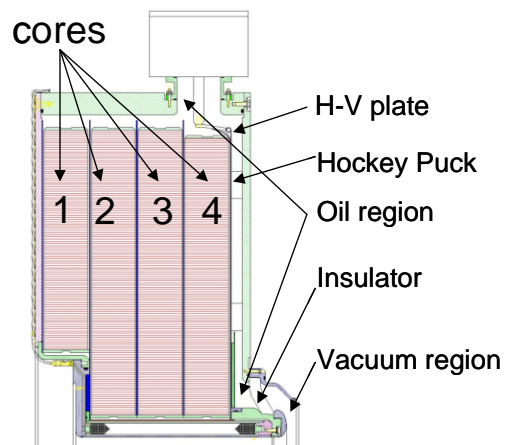


Figure 1: The cross-section of the original DARHT II induction cell design.

### CELL OIL REGION

In order to study the cell oil region, the vacuum region of the cell was filled with oil. Oil region testing was performed at LANL. The predominance of breakdowns in the upper quadrant of the cell raised the specter of problems with bubbles in the oil and attention to detail in oil processing and careful preparation of surfaces. Early experiments focused on the improvement of cell details and oil processing to improve high voltage performance.

Modeling efforts were undertaken to better understand electric field distributions in the cell oil region. The results of calculations and early experiments with cell detail modification led to the global modification of cell electric fields by extending the cell length.

#### Modification of Cell Oil Region Details

The original solid insulation between cores consisted of multiple layers of Mylar. The ~70-inch diameter cores were wound from 0.8 mil Metglas tape insulated with a layer of 0.2 mil Mylar. The Mylar layer extends ~0.05 inches on each side beyond the width of the 4-inch wide Metglas. A core contains ~20,000 turns of the Metglas with each turn separated by a layer of Mylar. The layers

\* This work was supported by the US National Nuclear Security Agency and the US Department of Energy under contract W-7405-ENG-36

‡ SAIC, Los Alamos, NM 87545, U.S.A.

† LANL, Los Alamos, NM 87545, U.S.A.

# LBNL, Berkeley, CA 94720, U.S.A.

♦ SAIC, Alamo, CA 94507, U.S.A.

■ ATK-MR, Albuquerque, NM 87110, U.S.A.

of Mylar contact the Mylar sheets that separate the cores. This area and the region between core-separating Mylar sheets create potential air bubble traps in the oil region.

Additionally, the layers of Metglas have a tendency to telescope and create localized field enhancements. The edges of stainless steel bands along the outer edge of the cores were also a source of localized field enhancement.

Extensive efforts were undertaken to reduce the likelihood of air bubbles in the oil and to reduce localized field enhancements. The multiple Mylar sheets were replaced with a single 60-mil thick sheet of high-density polyethylene. Radial slats were used between cores to improve oil circulation. Efforts were made to reduce core telescoping, corner radii were increased and electrical surfaces polished. These efforts improved the cell performance, but were found to be inadequate to reliably meet specifications.

### Cell Oil Region Extension

Four modeling efforts were undertaken to understand electric field distribution within the oil region of the cell. The four include a time dependent electromagnetic model [4], an analytical model [5], an electrostatic model, and a capacitive ladder circuit model. All of these models reinforced each other and revealed higher than expected electric fields between the outer edge of core 4 and the high voltage plate, and between core 4 and core 3. Figure 2 shows results from the electromagnetic model. These calculations showed that the core-to-core capacitance was much smaller than expected, and the core-to-housing stray capacitance was comparable to the core-to-core capacitance, resulting in an uneven voltage distribution between cores. The reason for the lower than expected core-to-core capacitance is that the radial Metglas layer-to-layer capacitance and the axial core-to-core capacitance constitute a capacitive ladder line. The result is an effective core-to-core capacitance involving only an inch or so of the outer edge of the core face where the potential difference to the adjacent core is highest.

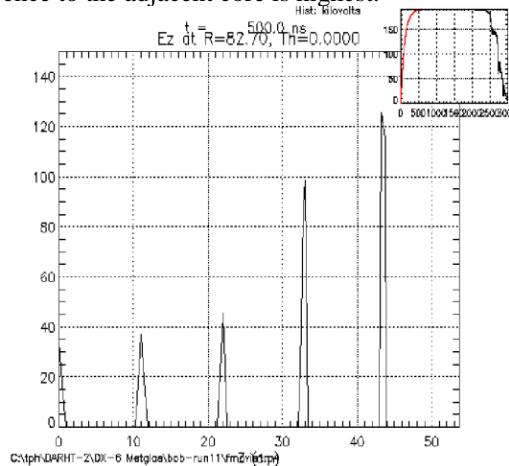


Figure 2: Calculation of the Electric Fields at the outer edge of the cores as a function of axial position. The highest field ~125 kV/cm occurs between core 4 and the high voltage plate.

The stray capacitance from core-to-housing pulled down the potential on the outer edge of the cores and resulted in a very high potential difference between the high voltage plate and the outer edge of core 4, and between the outer edge of core 4 and the outer edge of core 3. Extending the gap between core 4 and the high voltage plate reduced the fields in this region to roughly the levels experienced between each core.

Increasing the distance between core 4 and the high voltage plate from the original 0.25 inches to 1.0 inch reduced the calculated peak fields by nearly a factor of 4 and also reduced the other core-to-core fields by a substantial factor. These calculations were verified in a small-scale test where core-to-core potentials could be measured directly. Figure 3 shows the resultant fields with and without extension measured on the small-scale test.

Gradient distributions (normalized to voltage) per gap for 4-Core Small-scale Test at LBNL

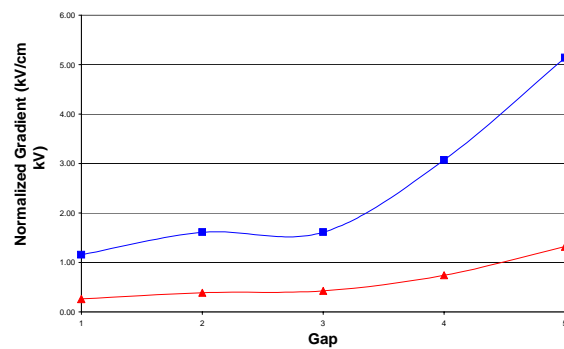


Figure 3: Normalized gradient (kV/cm-kV) measured in a small-scale mock-up of the cell. The upper trace is without extension and the lower trace demonstrates field reduction due to extension.

### Hockey Puck Extension

The extension of the cell provided ample room to increase the length of the high voltage plate to endplate standoffs or hockey pucks. Recesses were stamped in the high voltage plate and pockets were machined in the end plate, which increased the hockey puck length from 1.0 inch to 1.5 inches. A cross section of the cell is shown in Figure 4, where the recesses that allow hockey puck extension and reduce the fields at the end of the pucks are shown.

As Figure 4 shows, the cell housing length is increased by the addition of a 1-inch thick ring on the outer diameter and the addition of a 1-inch thick ring on the inner diameter [6]. To fill up the additional length in the oil volume, 1-inch poly-spoke spacers are placed between core 4 and the high voltage plate. The extended cell oil region has been pulsed for over 150,000 pulses on a total of 7 different cells at voltages between 220 kV and 250 kV; It has also been pulsed over 25,000 pulses at 300 kV, all without any high voltage breakdowns. The cell is specified to operate at 200 kV.

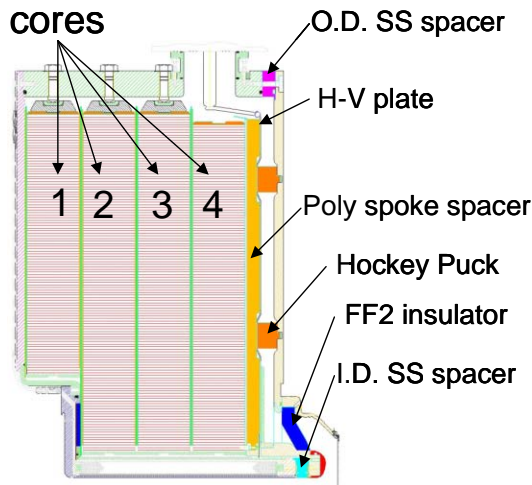


Figure 4: A cross-section of the upper oil region of the extended cell.

### CELL VACUUM REGION

In order to independently test the cell vacuum region, a cell vacuum region mock-up, in which a cell vacuum insulator could be mounted, was added to the NTX Beam line at LBNL. The NTX beam line is powered by a Marx generator that could deliver >10-microsecond 340 kV pulses to the insulator under test. A crowbar was used to set the pulse length at 2-3 microseconds. The DARHT II requirement for the cell pulse length is 2 microseconds. This set-up was referred to as the Insulator Test Stand (ITS). Once the extended cell oil region was demonstrated to be highly reliable, insulator designs were also tested on an extended cell at both LBNL and LANL. Testing included such issues as venting the vacuum region under various cleanliness scenarios to determine operational constraints. Figure 5 shows the calculated equal potential lines for the original baseline design.

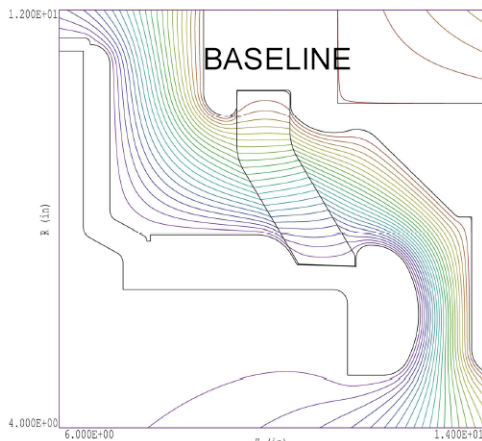


Figure 5: The calculated equal potential lines for the original baseline vacuum insulator design.

Electrostatic calculations were undertaken to examine the field distribution along the insulator and in the accelerating gap. A finer mesh size than used in the original design effort revealed more peaking of the field in the anode triple point region and the cathode triple

point region than previously reported [7]. At the cathode end, the field lines were angled such that electrons leaving some portions of the cathode could intersect the insulator. Various conceptual calculated designs were proposed to reduce fields at both the cathode and anode ends of the insulator and to correct field angles at the cathode end. The first test of one of these concepts to be tested on the ITS was referred to as Flatface 1.

### Flatface 1

Flatface 1 (FF1) was produced primarily to test proposed electrical concepts. FF1 was a modification of the original insulator design and featured a continuous flat profile from the anode to the cathode. FF1 had a large gap between the insulator and anode shield, which reduced the field peaking in the anode triple point region, and a revised cathode triple point region that reduced fields and corrected field angles to carry electrons away from the insulator. A cross-section of FF1 with its calculated equal potential lines is shown in Figure 6.

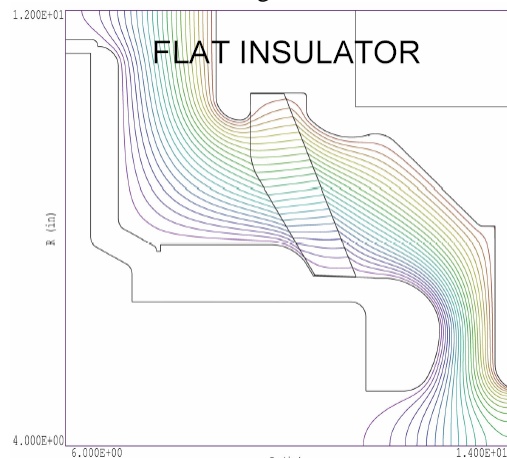


Figure 6: A calculation of the equal potential lines for Flatface 1 (FF1), which featured modifications of the original baseline design at both the anode end and the cathode end. Additionally, the cathode cap was modified as shown.

When tested on the ITS, FF1 was pulsed at increasing voltages up to the limit of the test stand (340 kV) and operated there for over a thousand pulses with no failures. The problem with the FF1 design is that the reduction of cross-section in the anode region reduced its mechanical strength, making it unsatisfactory for use on a cell.

### Flatface 2

Flatface 2 (FF2) was originally tested to determine whether the cathode region modifications of FF1 would improve the original design without mechanical strength reductions incorporated into the anode region of FF1. FF2 would answer the question concerning the importance of the cathode region modifications to the original design as compared to anode region modifications to the original design. Figure 7 shows a cross section of the FF2 design and calculated equal potential lines. Figures 8 & 9 show the reduction in the peak electrical field near the cathode

and the reversal of field angles from negative to positive values. The figures also demonstrate the similarity of FF1 (Flat Insulator) and FF2 (New Design) at the cathode end.

The FF2 performed as well on the ITS as FF1. It was tested up to 340 kV for over a thousand  $\leq 3$  microsecond pulses without any breakdowns. Other insulator designs were also the subject of testing, but they were plagued by mechanical assembly problems and robustness problems. FF2 met and exceeded requirements in all tests to which it was subjected.

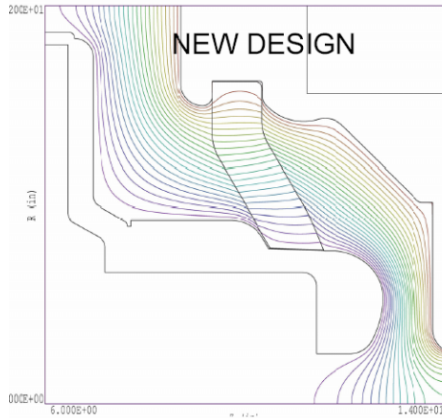


Figure 7: Calculated equal potential lines for FF2 the new baseline design for the DARHT II refurbishment project.

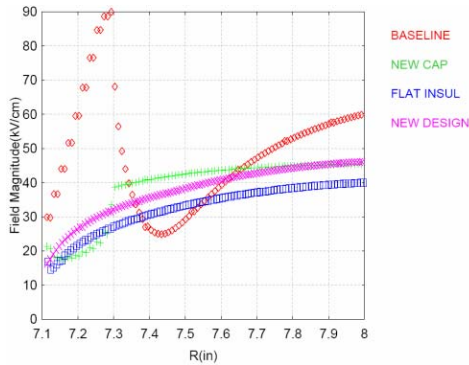


Figure 8: Reduction in electric field peaking along insulator surface near the cathode triple point comparing the original baseline with alternate designs and the new design.

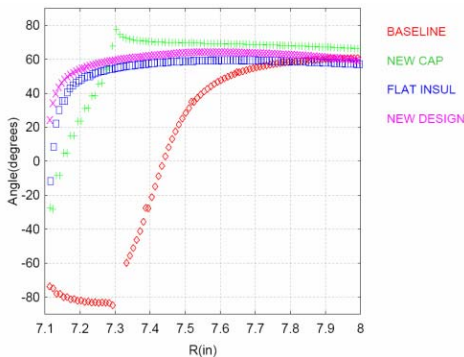


Figure 9: A comparison of field angles along insulator surface showing proper angles in the new design as compared with reversal to negative values near the cathode in original baseline.

### Diode Boards

The design of FF2 does not address the peaking of the field at the anode triple point region. This becomes an issue during the reversal when the anode effectively becomes the cathode. Since vacuum breakdowns had been frequently observed during reversal, the anode region had to be addressed. This was accomplished by clamping the reversal of the cell with a diode string mounted in the PFN. Figure 10 shows the waveform including reversal with the original PFN design. Figure 11 compares the minimal reversal with the diode reversal clamping string in the PFN. Reversal occurs due to saturation of the Metglas cores late in the pulse.

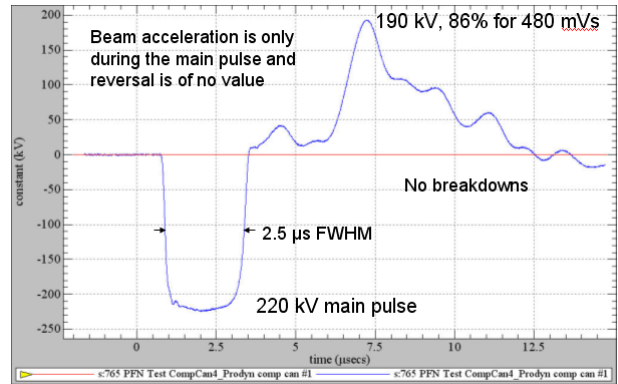


Figure 10: The voltage waveform for a 220 kV pulse showing a reversal of  $\sim 190$  kV or  $\sim 86\%$  in the original PFN configuration.

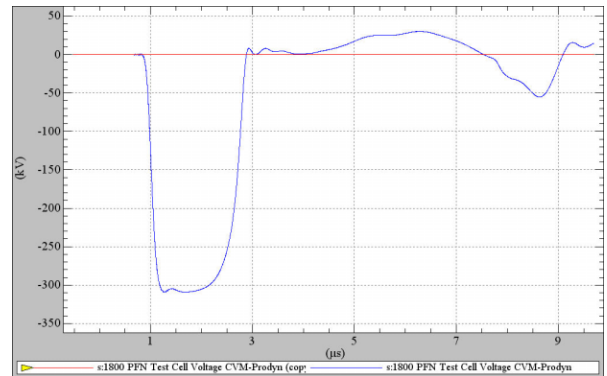


Figure 11: The voltage waveform for a 300 kV pulse showing a reversal of less than 40 kV or  $\sim 13\%$  using a PFN with reversal clamping diodes.

Using the diode string to eliminate reversal removed problems created by the anode region field peaking. This eliminated the need to modify the anode end of the insulator and made FF2 a viable solution to the vacuum insulator problem.

### Bulk Insulator Testing

One Mycalex insulator on the original 78-cell accelerator experienced bulk breakdown very early in its lifecycle. To test insulator limits, one unit was tested on a Marx Generator at LLNL with over 130,000 pulses at 400 kV without failure, and another two units were tested to

failure on a 1 MV Marx Generator at Titan PSD. One unit failed at 2.6 times the operating voltage, and the second unit failed at 4.6 times, demonstrating their soundness.

### ACCEPTANCE TESTING

Successful modification of the oil region utilizing the extended cell, and modification of the vacuum region utilizing FF2 led to integrated testing of the entire cell. An extended cell with FF2 was first assembled as a pre-prototype (PP-1) at LANL and tested for 15,200 pulses at 300 kV without any failures. Similar success was experienced at LBNL as part of the insulator testing with an extended cell. These successes led to the establishment of a new baseline design for the DARHT II Refurbishment and Commissioning project. To demonstrate the reliability of the new baseline, an acceptance-testing program was established that would statistically demonstrate the required reliability of the DARHT II cells. The test sequence is summarized in Table 1.

The acceptance tests allowed for a maximum of 8 faults to occur during the testing sequence to meet the required reliability. The acceptance testing has been completed, and no faults have occurred. In fact, the testing exceeded the required number of pulses on units 2-4 by over 3000 pulses. In addition, several of the acceptance test units were used for other tests after their sequence was completed, adding several thousand more pulses without a failure. Over 200,000 test pulses at voltages  $\geq 200$  kV and over 70,000 pulses at voltages  $>250$  kV were fired with no failures.

Table 1: Summary of the number of pulses, voltage levels and allowed number of failures to meet reliability requirements in the prototype design acceptance tests. No failures occurred during testing

| Prototype Unit   | Voltage Test Level | # Shots | Acceptable Result        |
|--|--------------------|---------|--------------------------|
| #1   | 200 kV             | 50,000  | No catastrophic failures |
|  |                    |         | No more than one failure |
| #2   | 220 kV             | 25,000  | See Note 1               |
|  | 250 kV             | 8,700   | See Note 2               |
| #3   | 220 kV             | 25,000  | See Note 1               |
|  | 250 kV             | 8,700   | See Note 2               |
| #4   | 220 kV             | 25,000  | See Note 1               |
|  | 250 kV             | 8,700   | See Note 2               |
| #5   | 250 kV             | 8,700   | See Note 2               |
| #6   | 250 kV             | 8,700   | See Note 2               |
| Total # of Cell Shots  |                    | 168,500 |                          |
| Note 1. No more than 3 failures in the 75,000 shots taken at 220 kV. |                    |         |                          |
| Note 2. No more than 5 failures in the 43,500 shots taken at 250 kV. |                    |         |                          |

The acceptance test sequence has demonstrated that the new cell baseline for the DARHT II refurbishment project exceeds its required specifications.

### CONCLUSION

The original DARHT II accelerator cells' design experienced shortcomings in both the oil and vacuum regions. An R&D program was conducted to address both the oil and vacuum regions. The problems in the oil region have been solved by extending the cells, extending the hockey pucks, increasing the spacing between core 4 and the high voltage plate, and attention to detail to eliminate air bubbles and field enhancements. Modifying the vacuum insulator to a FF2 geometry and clamping reversal with diode strings in the PFN have addressed the vacuum region problems. Bulk breakdown has been examined and determined to be an infant mortality question that is being addressed with aggressive acceptance testing.

Statistically significant acceptance testing of the revised cell baseline design has demonstrated that the new design exceeds its required specifications. This revised cell design is the basis of the DARHT II Refurbishment and Commissioning project.

### REFERENCES

- [1] Burns, M. J. et. al., "Status of the DARHT Phase 2 Long-Pulse Accelerator," PAC2001, Chicago, IL, June 2001, p.325
- [2] Metglas 2605 SC, a product of Metglas Inc.
- [3] Mycalex, a product of Crystex Composites LLC.
- [4] Hughes, T. P. et. al., "Numerical Model of the DARHT Accelerating Cell," poster FPAT033, this meeting.
- [5] Briggs, R. J, and Fawley, W. M., "A Simple Model for Induction Core Voltage Distributions, DARHT Technical Note No. 418, June 25, 2004
- [6] Barraza, J. et. al., "Mechanical Engineering Upgrades to the DARHT-II Induction Cells," 15th IEEE Pulse Power Conference, Monterey, CA, June 2005
- [7] Rutkowski, H. L. et. al., "A Long Pulse Linac for the Second Phase of DARHT" PAC1999, New, York, p. 21